

# Half-Loop Segmented Antenna with Omnidirectional Hemispherical Coverage for Wireless Communications

Payam Nayeri<sup>1</sup>, Atef Z. Elsherbeni<sup>1</sup>, Roger Hasse<sup>2</sup>, and Darko Kajfez<sup>3</sup>

<sup>1</sup>Department of Electrical Engineering and Computer Science  
Colorado School of Mines, Golden, CO 80401, USA  
pnayeri@mines.edu, aelsherb@mines.edu

<sup>2</sup>Georgia Tech Research Institute  
Georgia Institute of Technology, Atlanta, GA 30332, USA  
roger.hasse@gtri.gatech.edu

<sup>3</sup>Department of Electrical Engineering  
University of Mississippi, University, MS 38677, USA  
eedarko@olemiss.edu

**Abstract** — Segmented antennas loaded with reactance elements at the junctions between segments provide additional parameters for shaping antenna characteristics. The design procedure consists of first, circuit analysis of the multiport antenna description to determine the initial values of the lumped element reactances and second, of fine tuning the antenna dimensions full-wave simulation software. Measured results show that a good matching and an omnidirectional radiation pattern in the vertical plane is maintained up to  $\theta = 70^\circ$  with a circular ground plane of 1m diameter.

**Index Terms** — Antenna directivity, antenna impedance matrix, design optimization, omnidirectional antenna, partitioned antenna, printed circuit antenna, segmented antenna.

## I. INTRODUCTION

Many applications of wireless communication require antennas that provide omnidirectional radiation patterns. For example, an antenna designed for communication with non-stationary low-earth-orbit satellites should display an omnidirectional pattern in the upper half plane of a spherical system of coordinates. One possibility of creating such a radiation pattern is with the use of a half-loop segmented antenna [1] that can easily be fabricated in a printed-circuit form. As this antenna creates a linearly polarized field, a combination of two orthogonal antennas driven in a phase quadrature would be necessary for achieving circularly polarized radiation. This paper presents a new design of segmented half loop antenna that achieves omnidirectional radiation above a ground plane in one azimuthal plane.

The need for segmentation can be best understood by considering the characteristics of a solid (unsegmented) antenna such as shown in Fig. 1. We assume that the antenna circumference  $2a$  is approximately one-half wavelength, and the two generators are in phase opposition. A transmitting loop antenna placed above a perfectly conducting ground plane as shown in Fig. 1, produces the same field in the upper half-space as another double-sized, full-loop antenna, located in free space. To distinguish the antenna in Fig. 1 from other loop antennas, we will call it a *half-loop* antenna.

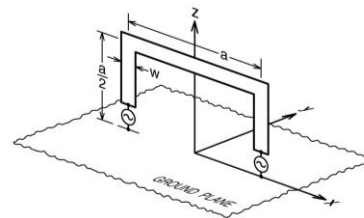


Fig. 1. A solid half-loop antenna above a perfectly conducting ground plane.

The directivity pattern created by such antenna is well known in the literature as is not shown for brevity. This pattern differs significantly from an ideal radiation pattern produced by an elementary magnetic dipole placed in the horizontal direction. In particular the directivity pattern of such an antenna drops by 5 decibels already at an angle of  $\theta = 60^\circ$ , instead of being constant up to the horizon as in the case of the elementary dipole. Note that in spherical system of coordinates, angle  $\theta$  is counted from the vertical  $z$  axis. On the other hand, when the half-loop antenna of the

same overall dimensions is partitioned into 7 total segments, separated by lumped reactances, the simulated radiation pattern becomes as shown in Fig. 2, which is almost identical with an ideal magnetic dipole pattern. In addition, the segmented antenna is better matched than the solid version. More details about the segmentation procedure will be provided in Section III. This pattern has been obtained by the use of the full wave EM simulation software Ansys HFSS [2], assuming an infinite ground plane.

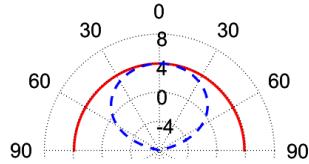


Fig. 2. Simulated directivity patterns of half-loop segmented antennas. The solid and dashed lines correspond to the  $xz$  and  $yz$  planes, respectively.

## II. EQUIVALENT CIRCUIT OF THE HALF-LOOP SEGMENTED ANTENNA

For a half-loop antenna with electrical length no greater than one-half wavelength, the radiation pattern could be made omnidirectional in the orthogonal plane, if one could maintain a stationary phase of the current distribution along the antenna conductor. The control of the current distribution along the antenna will be accomplished by segmenting the half-loop antenna into 7 segments as shown in Fig. 3. Without the loss of generality, the substrate used for the loop is a 32 mil Rogers RO4003 laminate.

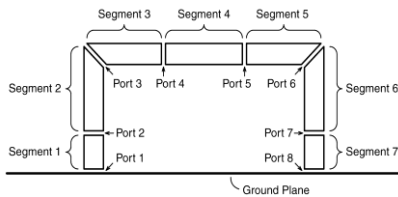


Fig. 3. The conductor of a half-loop antenna in Fig. 1 is divided into 7 segments.

Between each two neighboring segments a lumped reactance will be inserted leading to an equivalent circuit as shown in Fig. 4. From the circuit theory point of view, we see two impedance matrices; the antenna is described by matrix  $\mathbf{Z}_a$  while the “external” reactances constitute diagonal impedance matrix  $\mathbf{Z}_{ex}$ :

$$\mathbf{Z}_{ex} = \text{diag}(0, jX_2, jX_3, \dots, jX_7, 0). \quad (1)$$

The capacitive reactances are negative, and inductive reactances are positive. In order to insure that the radiation in the positive  $x$  direction is of the same intensity as the one in the negative  $x$  direction, the

reactance values should be made symmetric around the  $z$  axis, i.e.,  $X_2=X_7$ ,  $X_3=X_6$  and  $X_4=X_5$ . Furthermore the source voltages should be made equal to each other ( $V_{g1} = V_{g8}$ ). Then, the two input impedances will be equal to each other ( $Z_{in1} = Z_{in8}$ ), and the two powers delivered to the antenna ports will also be equal to each other ( $P_{in1} = P_{in2}$ ). Considering the structure in Fig. 3 to be an array comprised of 7 elements, the impedance matrix  $\mathbf{Z}_a$  can be generated using full-wave electromagnetic simulation software [2].

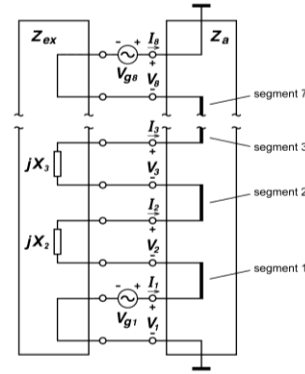


Fig. 4. Equivalent circuit of the half-loop segmented antenna.

When the voltages at the individual ports are grouped in the vector  $|V\rangle$  and the port currents in a vector  $|I\rangle$  the network in Fig. 4 is described by:

$$|I\rangle = (\mathbf{Z}_a + \mathbf{Z}_{ex})^{-1} |V_g\rangle. \quad (2)$$

The first component of vector  $|V_g\rangle$  is equal to  $V_{g1}$  and the 8<sup>th</sup> component is equal to  $V_{g8}$  while the rest of components are being equal to zero. For the operation in the phase opposition,  $V_{g1} = V_{g8}$ , and it is therefore possible to evaluate the voltages and currents at all the ports. Thus, for any combination of reactances  $X_2$  to  $X_7$  it is possible to determine the *exact* input impedance with the use of circuit-theory Equation (2), without the need to refer to a full wave simulation software. Furthermore, it is also possible to *approximately* compute the radiation pattern based on the results obtained by the circuit theory as follows. Each of the segments is considerably shorter than the free-space wavelength, so one can assume that the current distribution along an individual segment will not display significant fluctuations. Thus, it is reasonable to assume that the current on the segment  $i$  is equal to the average value of port currents entering and exiting that segment:

$$I_{si} = (I_i + I_{i+1}) / 2. \quad (3)$$

The antenna system in Fig. 3 can be viewed to represent an array of known linear current sources  $I_{si}$ , so

that it is possible to evaluate the total radiated field using antenna theory [3]. It is convenient to define current moments as follows:

$$I_{mi} = \frac{2\pi d_i}{\lambda} I_{si}, \quad (4)$$

where  $d_i$  is the length of the segment  $i$  and  $\lambda$  is the free space wavelength. When the segments  $i$  ( $i = 1$  to  $7$ ) are rotated by angles  $\gamma_i$  with respect to the  $z$ -axis, their centers being located in the  $xz$ -plane at coordinates  $x_i$  and  $z_i$ , the general formula for directivity in the  $xz$  plane becomes:

$$D(\theta) = \frac{7.5}{P_{inl}} \left| \sum_{i=1}^{14} I_{mi} \sin(\theta - \gamma_i) e^{jk(x_i \sin \theta + z_i \cos \theta)} \right|^2. \quad (5)$$

Figure 5 displays the individual current moments that are used for computing the directivity. Although there are only 7 physical segments on the antenna, there are also 7 images below the ground plane that must be added in the summation (5). It is important to note that the number of segments needed for any given design is subjective. In the proposed design initially 5 segments were considered, however it was observed that adding segments on the top corners were necessary, hence this number was increased to 7. While adding more segments is also possible, due to added complexity it should generally be avoided.

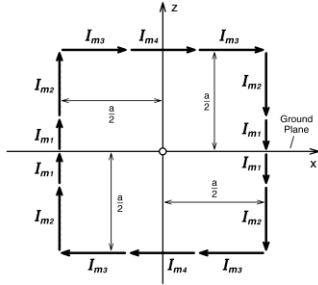


Fig. 5. The positions and orientations of the current moments on the segmented half-loop antenna.

### III. OPTIMIZATION PROCEDURE FOR INDIVIDUAL REACTANCES

Expression (5) enables one to estimate the radiation pattern as a function of  $\theta$ . For optimization purposes, directivity  $D$  is evaluated at a number of  $\theta$  points. Afterwards, the mean value  $mD$  and the standard deviation  $sD$  of all the points are computed. The objective function for optimization is then selected to be:

$$U = \frac{w_1}{mD} + w_2 \cdot sD + w_3 \cdot \rho. \quad (6)$$

In this way, the mean directivity is maximized, the standard deviation of directivity (i.e., the departure from the omnidirectional shape) is minimized, and the input reflection coefficient is minimized. The weight  $w_1$  is used to emphasize the mean directivity;  $w_2$  is used to emphasize the uniform directivity; and  $w_3$  is used to

emphasize the impedance match.

For demonstration and verification purposes, the side length of the half-loop from Fig. 6 is selected to be  $a = 62$  mm, and the strip width is 5 mm. The operating frequency is selected to be  $f = 1.2276$  GHz (GPS L2 band). The 8-port antenna impedance matrix is created by HFSS, while the initial optimization is performed with the Matlab® program “fminsearch” [4].

At the start of optimization, all reactances are set to be equal to  $-259 \Omega$  (i.e., 0.5 pF). The three optimized reactances come out to be  $X_2 = -500 \Omega$ ,  $X_3 = 92.7 \Omega$  and  $X_4 = -432 \Omega$ . Thus, the second and the fourth loading reactances are capacitive, while the third one is inductive. The amplitudes and phases of the current moments at the start of optimization are shown in Fig. 6 (a), and after optimization they are shown in Fig. 6 (b). It can be seen that the amplitudes of the current moments after optimization have become several times larger, because of an improved impedance match. The phase distribution has also changed somewhat after optimization, but phases still remain close to each other. The predicted mean directivity is  $mD = 3.6$  dBi, and the predicted input return loss is 20 dB.

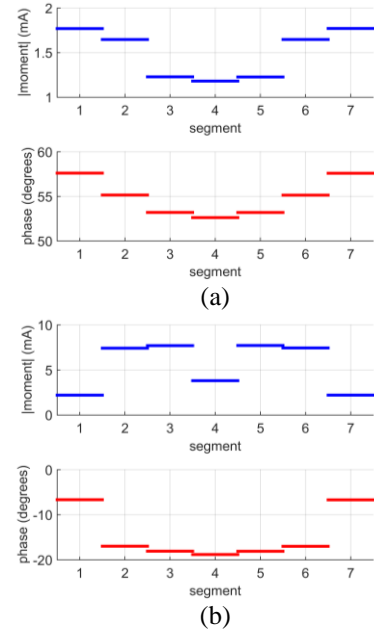


Fig. 6. Amplitudes and phases of current moments on individual segments: (a) before optimization, and (b) after optimization.

When the optimized values of lumped reactances are inserted in the antenna model, the radiation pattern obtained by HFSS is shown in Fig. 2 (b). As expected, the shape of the pattern closely resembles that of an ideal magnetic moment oriented along the  $y$  axis. As far as the directivity of this oversized magnetic dipole is concerned, the directivity value computed by HFSS is

slightly larger than the 3.6 dBi predicted by circuit analysis, namely 4.1 dBi in the z direction, and it drops to 3.8 dBi in the x direction. The simulated return loss is approximately 21.6 dB at 1.2276 GHz, which is in good agreement with the value obtained by circuit theory of 20 dB at 1.2276 GHz.

The final step is to model the required reactances of the segmented antenna. The inductance corresponding to  $X_3$  is  $L_3=12.03$  nH. This value is realized by a small circular loop in each of the two corners of the half-loop. The trace width for this inductor was set to 1 mm. The other two lumped elements are capacitances 0.26 and 0.30 pF, which are realized by overlapping the strips located on the opposite sides of the substrate. For these three sets of printed reactive elements, the initial dimensions were determined based on static approximation. The final dimensions, i.e., the loop radius for the inductors and overlap length for the capacitors, were determined with direct optimization of these parameters in the full-wave software. This secondary optimization resulted in an omnidirectional directivity of 3.8 dBi in both x and z directions, with the input reflection coefficient magnitude of -21.6 dB at 1.2276 GHz. The dimensions for the inductive loop radius, and the overlap capacitor lengths, were 2.22 mm, 1.55 mm, and 1.95 mm, respectively. The printed circuit arrangement, and a photo of its prototype, are shown in Fig. 7. A lumped port excitation was used in the simulation model to represent the SMA end-launch connector of the fabricated prototype. The substrate used for the ground plane and feed network is a 62 mil Rogers RT/Duroid 5880. Note that the feed network is a power divider which feeds the two ports of the HLA out of phase [1].

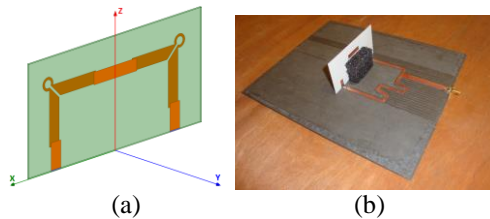


Fig. 7. (a) Printed circuit version of the antenna. (b) Half-loop segmented antenna prototype.

#### IV. PROTOTYPE MEASUREMENTS

The radiation pattern measured with a ground plane of 1 meter diameter is compared with the simulated pattern in Fig. 8. The antenna radiation pattern and efficiency were measured using the SG64 Starlab measurement system at Kennesaw, GA. Because of the limited ground plane size, the edge diffraction effect is clearly visible. The measured value drops below the simulated value at  $\theta = 70^\circ$ . For a larger ground plane size, one would expect wider omnidirectional coverage

angle. The measured radiation efficiency at the center frequency is 93%. The measured reflection coefficient magnitude is given in Fig. 9.

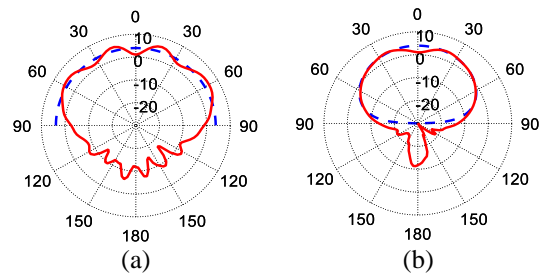


Fig. 8. Measured (solid) and simulated (dashed) radiation patterns of the antenna at 1.2276 GHz in: (a)  $xz$  or  $\phi = 0^\circ$  and (b)  $yz$  or  $\phi = 90^\circ$  planes.

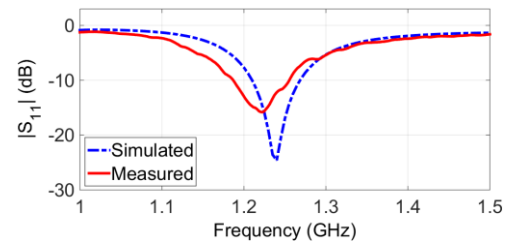


Fig. 9. Reflection coefficient magnitude of the antenna.

#### V. CONCLUSIONS

By allowing the individual reactances in a segmented antenna to take distinct values, it becomes possible to simultaneously optimize the radiation pattern and the input match of the antenna. A preliminary optimization is considerably speeded up by analyzing the antenna equivalent circuit. The required capacitances and inductances can be easily integrated into the printed circuit of the segmented antenna, such that no external matching circuit is necessary.

#### ACKNOWLEDGMENT

The authors would like to thank Microwave Vision Group (MVG) and Satimo USA for the measurement of segmented antennas using the SG64 Starlab system at Kennesaw, GA, and to Ansys Inc. for their software package donation to Colorado School of Mines.

#### REFERENCES

- [1] P. Nayeri, D. Kajfez, and A. Z. Elsherbeni, "Design of a segmented half-loop antenna," *IEEE Antennas and Propagation Society International Symposium*, Memphis, TN, July 2014.
- [2] ANSYS HFSS, v. 15.0, ANSYS Inc.
- [3] R. E. Collin, *Radiation from Simple Sources*, Ch. 2, Antenna Theory, Part I, New York: McGraw-Hill, 1969.
- [4] Matlab®, The Mathworks Inc., Natick, MA.